CrystEngComm

RSC Publishing

PAPER

View Article Online
View Journal | View Issue

Cite this: *CrystEngComm*, 2013, **15**, 1365

Growth and microstructure of heterogeneous crystal GaSe:InS

Victor V. Atuchin,*[a] Nina F. Beisel,[b] Konstantin A. Kokh,[c] Vladimir N. Kruchinin,[d] Ilya V. Korolkov,[e] Lev D. Pokrovsky,[a] Alphiya R. Tsygankova[b] and Aleksander E. Kokh[c]

Received 12th September 2012,
Accepted 26th November 2012

DOI: 10.1039/c2ce26474a

www.rsc.org/crystengcomm

An optical quality GaSe:InS single crystal has been grown by modified Bridgman technique using nonstationary temperature distribution for effective melt mixing. The phase composition of the crystal has been verified with XRD and TEM. The chemical composition variation along the crystal has been evaluated with electron probe microanalysis (EPMA), atomic-emission spectrometry with inductively-coupled plasma (ICP-AES) and atomic-absorption spectrometry (AAS). The joint solubility limits in the GaSe:InS system are measured as y_{In} = 0.28 at% and y_S = 7 at%. The optical properties of GaSe:InS crystal have been obtained with spectroscopic ellipsometry (SE).

Introduction

The nonlinear optical crystal GaSe is a highly promising material used for frequency conversion over IR and THz spectral ranges.[1–4] It is well known that GaSe is capable of incorporating different doping elements at a high content with a noticeable modification of physical properties.[5–13] Up to now, many single-element dopants have been tested for incorporation into cation or anion sublattices of the GaSe crystal, and the solubility limits and real defect structure were estimated for several solid solutions. Besides, there were several attempts made to use complex doping in GaSe. The electrical properties of $GaSe_{0.95}S_{0.05}$:Na (4%) crystals grown by the Bridgman method were evaluated.[14] Compounds $AgGaSe_2$ and $AgGaS_2$ were used as complex dopants in GaSe.[5,12] As it was reported, the introduction of $AgGaSe_2$ (10.4% mass) into the initial charge resulted in the noticeable increase of nonlinear optical coefficient up to $d \sim 75$ pm V^{-1}.[5] The hardness increase, blue shift of the transparency cut edge and the noticeable variation of phase-matching angles were reported in GaSe:$AgGaS_2$ (10.6% mass) crystal without a loss of optical quality.[12] A detailed observation of growth conditions, final chemical composition and structural properties, however, was not made for these two crystals.

Up to now, better results have been achieved for GaSe doped with elemental S or In. The layered crystals GaSe and GaS have a similar atom arrangement in the layers and that provides a continuous set of the solid solutions $GaSe_{1-x}S_x$ with a possible formation of several polymorph modifications defined by the layer stocking.[15–18] The situation with indium incorporation into the GaSe lattice is less clear. Optical quality GaSe:In crystals are grown at a low In content.[5,8,11] At a higher In content, the growth of $Ga_{1-y}In_ySe$ single crystal with GaSe structure was possible only for the range of $0 \leqslant y \leqslant 0.25$ and, respectively, the solubility limit of In in GaSe can be estimated as $y \sim 0.25$ or 12.5 at% on the basis of crystal composition estimations made by neutron activation analysis.[19] Compared to that, as low In solubility as $y_{In} \sim 1.7$ at% was found in another experiment on $Ga_{1-y}In_ySe$ crystal growth when crystal composition was estimated by EPMA.[20] So, the available information on In solubility in GaSe is very contradictory. The present study is aimed at the crystal growth and complex evaluation of microstructural properties of $(GaSe)_{1-x}(InS)_x$ crystals. This is argued by common effective ion radii relations in this solid solution. Indeed, the lattice extension generated by isomorphous substitution of Ga^{3+} with larger In^{3+} ions may be compensated by lattice contrition due to the parallel substitution of Se^{3-} by a smaller S^{3-} ions. This mechanism may result in a higher solubility limit and better crystal quality.

Experiment

The starting materials for crystal growth were Ga (6N) and Se, In, S (5N). At the first stage, polycrystalline compounds GaSe

[a]*Laboratory of Optical Materials and Structures, Institute of Semiconductor Physics, SB RAS, Novosibirsk 90, 630090, Russia. E-mail: atuchin@isp.nsc.ru; Fax: +7 383 3332771; Tel: +7 383 3308889*
[b]*Analytical Laboratory, Nikolaev Institute of Inorganic Chemistry, SB RAS, Novosibirsk 90, 630090, Russia. E-mail: beisel@niic.nsc.ru; Fax: +7 383 3309489; Tel: +7 383 3306965*
[c]*Laboratory of Crystal Growth, Institute of Geology and Mineralogy, SB RAS, Novosibirsk 90, 630090, Russia. E-mail: k.a.kokh@gmail.com; a.e.kokh@gmail.com; Fax: +7 383 33066392; Tel: +7 383 33066392*
[d]*Laboratory for Ellipsometry of Semiconductor Materials and Structures, Institute of Semiconductor Physics, SB RAS, Novosibirsk 90, 630090, Russia. E-mail: kruch@isp.nsc.ru; Fax: +7 383 3332771; Tel: +7 383 3308946*
[e]*Laboratory of Crystal Chemistry, Nikolaev Institute of Inorganic Chemistry, SB RAS, Novosibirsk 90, 630090, Russia. E-mail: korolkov@niic.nsc.ru; Fax: +7 383 3309489; Tel: +7 383 3309466*

and InS were synthesized by the two zone method according to the technique described elsewhere.[21] Then, the polycrystalline presynthesized charges were put into a quartz ampoule in molar ratio GaSe : InS = 0.80 : 0.20. After evacuation up to 10^{-4} Torr, the ampoule was sealed off using a propane–oxygen flame. Crystal growth was produced by the modified Bridgman technique.[22] The novel Bridgman furnace used in this experiment was equipped with the middle zone where nonstationary temperature distribution provides a more effective mixing in the melt, which is very important for multicomponent melts.[23] The GaSe:InS crystal was grown in the temperature range 935–850 °C, as measured at the bottom point of the ampoule. The duration of the growth process was 10 days. As a result, a crystal with the diameter of 7 mm and length of 100 mm was grown. The cleavage plane of the GaSe:InS crystal was found to be orthogonal to the growth direction that is quite a rare event for layered chalcogenide compounds.[5–8,10–13,20,24–28] Due to such orientation of the cleavage plane, the crystal was broken into several 15–30 mm pieces during cooling. A view through the cleaved faces of one such piece is shown in Fig. 1. The GaSe:InS boule grown was in a single-crystal state over the length of 0–40 mm from the seed, and the remaining part was polycrystalline.

The samples for measurements were cleaved from the grown ingot parallel to (001) and were used without an additional surface treatment. The structural properties were observed with XRD and TEM. XRD patterns were recorded using DRON-3M (Cu Kα radiation, Ni – filter, 5–60° 2θ range, 2 s per step) device (NPP Bourevestnik, Russia). A sample of GaSe:InS crystal was cut into 0.5 mm pieces and these were gently ground with hexane in an agate mortar and the resulting suspension was deposited on the polished side of a standard quartz sample holder, a smooth thin layer being formed after drying. Indexing the diffraction patterns was carried out using the data for the compounds reported in the PDF database [Powder Diffraction File. Alphabetical Index. Inorganic Phases, JCPDS, 1983 (International Centre for Diffraction Data, Pennsylvania, USA)]. TEM patterns were obtained from the flakes occasionally formed onto the cleaved (001) surface of the GaSe:InS crystal. The measurements were produced using a EFZ4 device (Carl Zeiss, Germany) at 50 keV electron energy.

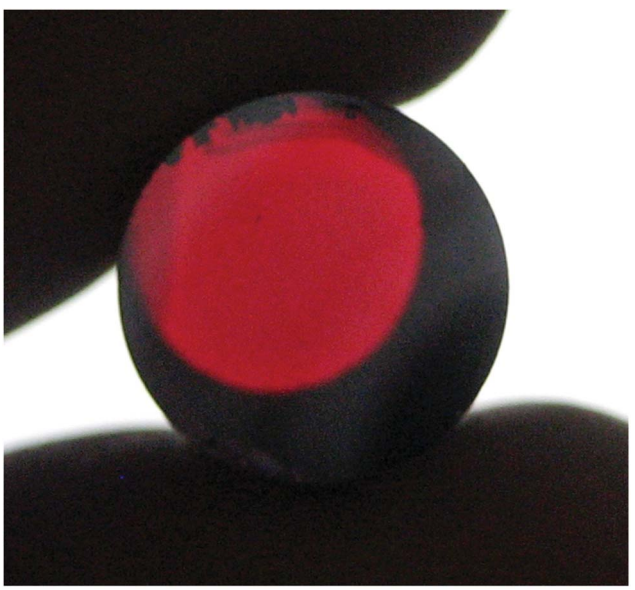

Fig. 1 GaSe:InS single crystal slightly illuminated by sunlight.

The chemical composition determination was provided with electron probe microanalysis (EPMA) using a JXA-8100 (JEOL, Japan) device and, for the selected samples, with atomic spectral methods. The as-grown crystal ingot was cut perpendicular to the growth axis to have the cylinder samples of 4–5 mm in thickness. For the position of the sample, which composition is within the length of solidified ingot, the parameter g was used. The parameter is introduced as $g = M^*/M$, where M is the total mass of ingot and M^* is the mass of ingot part from the seed point up to the considered sample.[29] Precisely weighed quantities of GaSe:InS crystal were dissolved in diluted HCl and the solutions were analyzed. The atomic-emission spectrometry with inductively-coupled plasma (ICP-AES), enabling us to determine up to 30 elements with detection limits 10^{-4}–10^{-6} wt% and relative standard deviation (S_r) 0.05–0.15 was used for the determination of In and S. The measurements were conducted using Spectrometer iCAP-6500 (Thermo Scientific, USA) and the scandium internal standard was added to the analyzed solutions for accounting matrix effects. Atomic-absorption spectrometry (AAS) with atomization in an air–acetylene flame gives us the opportunity to control the dopant content with the relative random error no more than 0.01–0.02.[30] Using a Zeeman AA spectrometer Z-8000 (Hitachi, Japan), we determined In in GaSe:InS crystals. The absence of significant systematic error was verified by the technique of additions, as well as that of subsequent dilution, S_r was less than 0.02.

Spectral dependencies of refractive index $n(\lambda)$ and extinction coefficient $k(\lambda)$ were determined by means of spectroscopic ellipsometry (SE). Ellipsometric angles Ψ and Δ were measured as a function of λ in the spectral range ~250–1030 nm using an ELLIPS-1771 SA ellipsometer.[31] The instrumental spectral resolution was 2 nm, the recording time of the spectrum did not exceed 20 s and the angle of incidence of light beam on the sample was 70°. The four-zone measurement method was used with subsequent averaging over all the four zones. Ellipsometry parameters Ψ and Δ are related to the complex Fresnel reflection coefficients by the equation:

$$tg\Psi e^{i\Delta} = \frac{R_p}{R_s} \quad (1)$$

where R_p and R_s are the coefficients for p- and s-polarized lightwave. To calculate the dependencies of the refractive index $n(\lambda)$ and extinction coefficient $k(\lambda)$ on optical wavelength λ, the experimental data were processed using the model of air-homogeneous isotropic substrate. Thus, in the whole spectral range, the spectral dependencies of polarization angles were fitted for m points of the spectrum by minimiza-

tion of the error function

$$\sigma^2 = \frac{1}{m}\sum_{i=1}^{m}\left[\left(\Delta_{\text{exp.}} - \Delta_{calc.}\right)^2 + \left(\Psi_{\text{exp.}} - \Psi_{\text{calc.}}\right)^2\right] \quad (2)$$

Here, $\Psi(\lambda)$ and $\Delta(\lambda)$ were also fitted using an approximate dispersion model proposed by Lorentz and Drude. According to this approximation, the dependence of the dielectric function on the photon energy can be represented as

$$\varepsilon(E) = \varepsilon_\infty - \frac{E_{1D}^2}{E^2 - iE_{2D}E} + \sum_{n=1}^{m}\frac{A_n E_n^2}{E_n^2 - E^2 + i\Gamma_n E_n E} \quad (3)$$

where E is the photon energy, eV, ε_∞ is the value of ε at $E \to \infty$, the second term in eqn (3) is the contribution from the Drude free carriers, and E_{1D} and E_{2D} are the constants. The interband transitions are described by the third Lorentz term on the basis of damped harmonic oscillators, and A_n, E_n, and Γ_n are the force, energy, and broadening function of an n-th oscillator from m oscillators included in the calculations.[32]

Results and discussion

The cleaved sample surface was found to be formed by wide flat terraces with sharp edges that are typical of the GaSe crystal surface. The presence of pure ε-GaSe-type crystal phase was verified by TEM and XRD analysis. The XRD curve recorded for the highly doped sample taken from the tail of crystalline part of the boule (g = 0.37) is shown in Fig. 2. The detected peaks are well matched to ε-GaSe, space group $P\bar{6}$, except for only one weak intensity feature at $2\theta = 20.11^\circ$.[33] The unit cell parameter c = 15.933 Å estimated for the peak at 2θ = 57.82° is in the wide range of c = 15.919–15.968 Å earlier observed in pure GaSe.[15,18,34–38] It is not possible to estimate the cell parameter a in XRD experiment because of a strongly preferential orientation of the crystal particles after grinding.

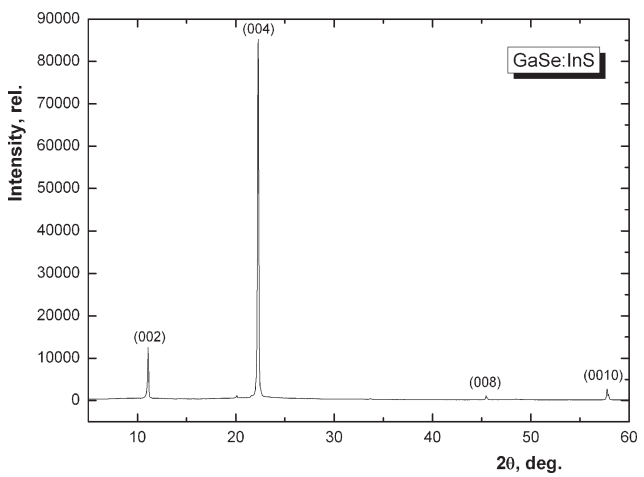

Fig. 2 XRD pattern obtained from GaSe:InS crystal.

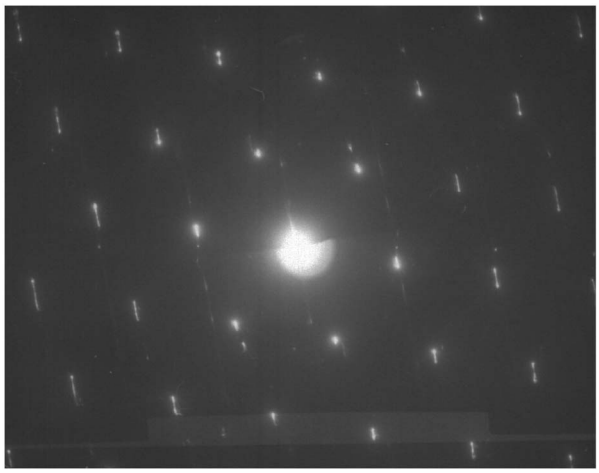

Fig. 3 SAED pattern recorded for cleaved GaSe:InS surface. Electron beam is along [001].

TEM observation produced for a suite of partly exfoliated crystal flakes indicates the presence of pure ε-GaSe-type crystal phase. As an example, the SAED pattern is shown in Fig. 3 when the electron beam is oriented along the polar direction [001] with the evident six-fold symmetry. The pattern is formed by several single-crystal flakes slightly rotated to each other. The unit cell parameters a = 3.78 and c = 15.96 Å estimated by TEM analysis are in good relation to the structural parameters of GaSe.[15,18,34–38]

Chemical composition analysis indicates the inhomogeneous distribution of In and nearly homogeneous distribution of S along the crystal growth direction with a higher In content at the crystal end. The distributions are shown in Fig. 4. The increase of the In doping level at the crystal end is verified by EPMA and ICP-AES. However, the values obtained by EPMA are evidently overestimated because of a low precision of EPMA at low element contents. The indium contents measured by the

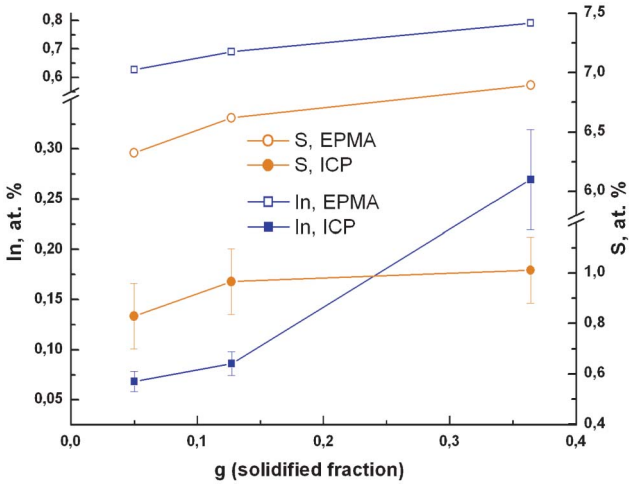

Fig. 4 Distribution of S and In over the GaSe:InS crystal.

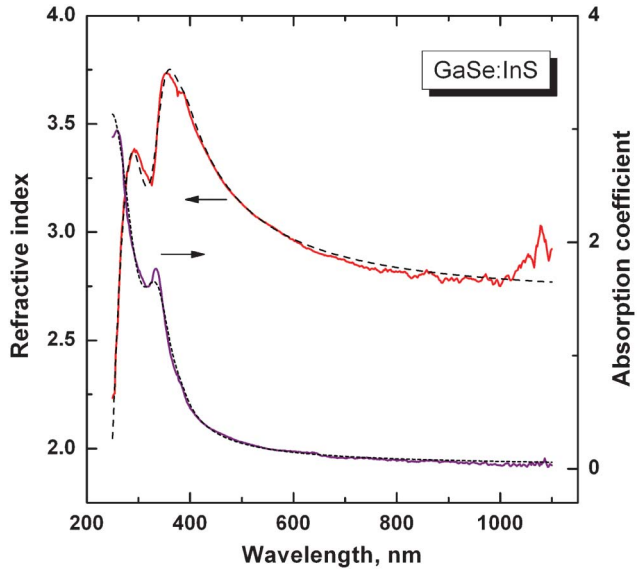

Fig. 5 Spectral dependencies $n(\lambda)$ and $k(\lambda)$ calculated for the GaSe:InS sample using spectral dependencies $\Psi(\lambda)$ and $\Delta(\lambda)$ (solid lines) and the dispersion Lorentz–Drude model (dotted lines).

ICP-AES method are excellently verified by AAS. So, the pronounced segregation of In can be stated in the GaSe:InS crystal. It should be pointed out that, In : S ratio in the grown crystal is varied in the range of 0.09–0.28 which is very far from that in InS. The highest indium concentration measured by ICP is 0.28 at%, which is lower than the data obtained by EPMA ($\sim$0.8 at%). Probably our result could be considered in agreement with that measured in ref. 20 by EPMA for $Ga_{1-y}In_ySe$ (1.7 at%), since EPMA has a large error for low element concentration. Thus, indium incorporation is a governing factor for both GaSe:In and GaSe:InS systems and that is less sensitive to the presence of sulfur.

In Fig. 5 the spectral dependencies of the refractive index and extinction coefficient are shown over the wavelength range λ = 250–1100 nm as it is determined for a sample with g = 0.13. The parameters of the Lorentz–Drude model are shown in Table 1. Generally, the shape of the curves $n(\lambda)$ and $k(\lambda)$ is very similar to those earlier obtained for GaSe:Te and $Ga_{0.75}In_{0.25}Se$ solid solutions, including the specific spectral feature at $\lambda \sim$ 335 nm.[10,11] Thus, a set of optical transitions in GaSe-type crystals was not varying drastically with doping.

Table 1 The Lorentz–Drude model parameters in GaSe:InS (g = 0.13)

ε_∞	E_{1D}	E_{2D}	A_1	E_1	Γ_1	σ
2.214	0.215	6.207	0.03	3.229	0.08	4.7
			A_2	E_2	Γ_2	
			1.424	3.644	0.189	
			A_3	E_3	Γ_3	
			1.012	4.539	0.228	
			A_4	E_4	Γ_4	
			2.622	4.879	0.165	

Conclusions

As it is shown by a crystal growth experiment, the optical quality crystals GaSe:InS can be grown at comparatively low doping levels. Initially it was supposed that the favourable relation of indium and sulfur effective ion radii will stimulate the substitution in the anion and cation sublattices of GaSe. Indeed, indium substitution for gallium should increase the unit cell volume because the effective radius of the In^{3+} ion is higher than that of the Ga^{3+} ion. This effect should be damped, at least partly, by the incorporation of small sulfur ions instead of large selenium ones. However, the supposition is not verified in the crystal growth experiment. Finally, structural parameters of highly doped GaSe:InS are found to be very similar to those of pure GaSe. It can be concluded that, generally, the presence of sulfur does not assist indium incorporation into the GaSe lattice. Thus, GaSe:InS crystals are the third heterogeneous system, together with $GaSe:AgGaSe_2$ and $GaSe:AgGaS_2$, able to provide optical quality crystals with tuned properties.

Acknowledgements

This study was partly supported by SB RAS under Project 46.12.

References

1 N. C. Fernelius, *Prog. Cryst. Growth Charact. Mater.*, 1994, **28**, 275.
2 N. B. Singh, D. R. Suhre, V. Balakrishna, M. Marable, R. Meyer, N. Fernelius, F. K. Hopkins and D. Zelmon, *Prog. Cryst. Growth Charact. Mater.*, 1998, **37**, 47.
3 W. Shi, Y. J. Ding, N. Fernelius and K. Vodopyanov, *Opt. Lett.*, 2002, **27**, 1454.
4 Y. Jiang and Y. J. Ding, *Appl. Phys. Lett.*, 2007, **91**, 091108.
5 N. B. Singh, D. R. Suhre, W. Rosch, R. Meyer, M. Marable, N. C. Fernelius, F. K. Hopkins, D. E. Zelmon and R. J. Narayanan, *J. Cryst. Growth*, 1999, **198–199**, 588.
6 A. Sh. Abdinov, R. F. Babaeva, R. M. Rzaev and G. A. Gasanov, *Inorg. Mater.*, 2004, **40**, 567.
7 Y. M. Andreev, V. V. Atuchin, G. V. Lanskii, A. N. Morozov, L. D. Pokrovsky, S. Y. Sarkisov and O. E. Voevodina, *Mater. Sci. Eng. B*, 2006, **128**, 205.
8 Z.-S. Feng, Z.-H. Kang, F.-G. Wu, J.-Y. Gao, Y. Jiang, H.-Z. Zhang, Y. M. Andreev, G. V. Lanskii, V. V. Atuchin and T. A. Gavrilova, *Opt. Express*, 2008, **16**, 9978.
9 M. Yüksek, A. Elmali, M. Karabulut and G. M. Mamedov, *Appl. Phys. B: Lasers Opt.*, 2009, **98**, 77.
10 S. Y. Sarkisov, V. V. Atuchin, T. A. Gavrilova, V. N. Kruchinin, S. A. Bereznaya, Z. V. Korotchenko, O. P. Tolbanov and A. I. Chernyshev, *Russ. Phys. J.*, 2010, **53**, 346.
11 M. Isik, S. S. Cetin, N. M. Gasanly and S. Ozcelik, *Solid State Commun.*, 2012, **152**, 791.
12 Y.-F. Zhang, R. Wang, Z.-H. Kang, L.-L. Qu, Y. Jiang, J.-Y. Gao, Y. M. Andreev, G. V. Lanskii, K. A. Kokh, A.

N. Morozov, A. V. Shaiduko and V. V. Zuev, *Opt. Commun.*, 2011, **284**, 1677.
13 Z.-H. Kang, J. Guo, Z.-S. Feng, J.-Y. Gao, J.-J. Xie, L.-M. Zhang, V. Atuchin, Y. Andreev, G. Lanskii and A. Shaiduko, *Appl. Phys. B: Lasers Opt.*, 2012, **108**, 545.
14 M. A. Osman, *Phys. B*, 2000, **275**, 351.
15 C. R. Whitehouse and A. A. Balchin, *J. Mater. Sci.*, 1978, **13**, 2394.
16 H. Serizawa, Y. Sasaki and Y. Nishina, *J. Phys. Soc. Jpn.*, 1980, **48**, 490.
17 C. P. León, L. Kador, K. R. Allakhverdiev, T. Baykara and A. A. Kaya, *J. Appl. Phys.*, 2005, **98**, 103103.
18 C. H. Ho, C. C. Wu and Z. H. Cheng, *J. Cryst. Growth*, 2005, **279**, 321.
19 G. Saintonge and J. L. Brebner, *Can. J. Phys.*, 1984, **62**, 730.
20 A. Gouskov, J. Camassel and L. Gouskov, *Prog. Cryst. Growth Charact.*, 1982, **5**, 323.
21 K. A. Kokh, Y. M. Andreev, V. A. Svetlichnyi, G. V. Lanskii and A. E. Kokh, *Cryst. Res. Technol.*, 2011, **46**, 327.
22 K. A. Kokh, B. G. Nenashev, A. E. Kokh and G. Y. Shvedenkov, *J. Cryst. Growth*, 2005, **275**, e2129.
23 K. A. Kokh, V. N. Popov, A. E. Kokh, B. A. Krasin and A. I. Nepomnyaschikh, *J. Cryst. Growth*, 2007, **303**, 253.
24 A. F. Qasrawi and N. M. Gasanly, *Solid State Commun.*, 2010, **150**, 325.
25 S. G. Choi, D. E. Aspnes, A. L. Fuchser, C. Martinez-Tomas, V. M. Sanjose and D. H. Levi, *Appl. Phys. Lett.*, 2010, **96**, 181902.
26 Y. M. Andreev, K. A. Kokh, G. V. Lanskii and A. N. Morozov, *J. Cryst. Growth*, 2011, **318**, 1164.
27 V. V. Atuchin, V. A. Golyashov, K. A. Kokh, I. V. Korolkov, A. S. Kozhukhov, V. N. Kruchinin, S. V. Makarenko, L. D. Pokrovsky, I. P. Prosvirin, K. N. Romanyuk and O. E. Tereshchenko, *Cryst. Growth Des.*, 2011, **11**, 5507.
28 M. Isik and N. M. Gasanly, *Cryst. Res. Technol.*, 2012, **47**, 530.
29 C. D. Thurmond, *The control of impurities in solids in Solid State Physics: Methods of Experimental Physics*, ed. K. Lark-Horovitz and V. A. Johnson, Academic Press Inc., London, 1959, vol. 6, part A.
30 I. G. Yudelevich, L. M. Buyanova, N. F. Beisel, L. A. Kozhanova, N. I. Petrova and I. Y. Vasiliev, *Izv. Sib. Otd. Akad. Nauk SSSR, Ser. Khim. Nauk*, 1984, **2**, 88.
31 S. V. Rykhlitski, E. V. Spesivtsev, V. A. Shvets and V. Y. Prokopiev, *Instrum. Exp. Tech.*, 2007, **2**, 160 in Russian.
32 K. Postava, M. Aoyama and T. Yamaguchi, *Appl. Surf. Sci.*, 2001, **175–176**, 270.
33 PDF files, Card [37–931].
34 J. C. J. M. Terhell and R. M. A. Lieth, *Phys. Status Solidi A*, 1971, **5**, 719.
35 M. K. Anis and F. M. Nazar, *J. Mater. Sci. Lett.*, 1983, **2**, 471.
36 K. Cenzual, L. M. Gelato, M. Penzo and E. Parthe, *Acta Crystallogr., Sect. B: Struct. Sci.*, 1991, **47**, 433.
37 C. C. Wu, C. H. Ho, W. T. Shen, Z. H. Cheng, Y. S. Huang and K. K. Tiong, *Mater. Chem. Phys.*, 2004, **88**, 313.
38 U. Schwarz, D. Olguin, A. Cantarero, M. Hanfland and K. Svassen, *Phys. Status Solidi B*, 2007, **244**, 244.